Journal of Photonics for Energy

PhotonicsforEnergy.SPIEDigitalLibrary.org

Theoretical insights into molecular blending on charge transport properties in organic semiconductors based on quantum nuclear tunneling model

Weitang Li
Zhigang Shuai
Hua Geng

SPIE.

Weitang Li, Zhigang Shuai, Hua Geng, "Theoretical insights into molecular blending on charge transport properties in organic semiconductors based on quantum nuclear tunneling model," *J. Photon. Energy* **8**(3), 032204 (2018), doi: 10.1117/1.JPE.8.032204.

Theoretical insights into molecular blending on charge transport properties in organic semiconductors based on quantum nuclear tunneling model

Weitang Li,[a] Zhigang Shuai,[a,*] and Hua Geng[b,*]
[a]Tsinghua University, MOE Key Laboratory of Organic Optoelectronics and Molecular Engineering, Department of Chemistry, Beijing, China
[b]Capital Normal University, Department of Chemistry, Beijing, China

Abstract. The effects of molecular blending on the charge transport properties of organic semiconductors are studied based on *ab initio* DFT calculation and quantum nuclear tunneling model coupled with kinetic Monte-Carlo simulation. Two model compounds, [(2,3,9,10-tetrachloropentacene-6,13-diyl)bis(ethyne-2,1-diyl)]bis(triisopropylsilane) (4Cl-TIPS-P) and [(1,2,3,4,8,9,10,11-octafluoropentacene-6,13-diyl)bis(ethyne-2,1-diyl)]bis(triisopropylsilane) (8F-TIPS-P), are blended homogeneously with different ratios, and the system is studied at a temperature ranging from 50 to 300 K. Our result shows that, at high temperature, blending leads to a smooth shift in mobility, whereas at a low temperature, one of the components tends to become traps, thus hamper the charge transport at low concentration. It is found that at 50 K, blending 0.995 mol. % of 4Cl-TIPS-P with 0.005 mol. % of 8F-TIPS-P, whose site energy is 48.1 meV lower than that of 4Cl-TIPS-P, would reduce the electron mobility by three orders of magnitude from that of pristine 4Cl-TIPS-P due to the trapping effect. The results are in agreement with the experimental observations. [DOI: 10.1117/1.JPE.8.032204]

Keywords: organic semiconductor; charge transport; hopping.

Paper 18008SS received Jan. 15, 2018; accepted for publication Mar. 19, 2018; published online Apr. 6, 2018.

1 Introduction

Over the past few decades, organic semiconductors have been widely studied, due to their potential application in the next generation of electronic devices. To optimize the performance of the devices and modulate the charge transport properties in organic semiconductors, scientists have developed various approaches, including introducing substitution groups,[1–3] doping,[4–6] adjusting symmetry,[7] improving manufacture techniques,[8,9] and so on. In 2016, inspired by inorganic semiconductors, Schwarze et al. first reported that band structure engineering could be achieved in organic semiconductors by blending organic small molecules, opening a new gate for design of organic semiconductors.[10] Theoretical description of the charge transport in blended organic semiconductors is a challenging issue. Understanding of the relationship between blend ratio and charge transport of devices is urgent for further development of organic semiconductors.

Blending effects on the charge transport properties of organic semiconductors can be quite complicated. Schwarze et al. ascribed the tuning effect to long-range Coulomb interactions.[10] Fong et al.,[11,12] Li et al.,[13] and Li et al.[14,15] studied the trapping and scattering effects for doped disordered organic semiconductors. Their simulation studies rely on either Gaussian disorder model (GDM)[16] or space-charge-limited current model with exponentially distributed traps, thus limited by parameter fitting and phenomenological explanation of the experimental measurements. The more ordered crystalline structure of the blending system also rules out a GDM

*Address all correspondence to: Zhigang Shuai, E-mail: zgshuai@tsinghua.edu.cn; Hua Geng, E-mail: hgeng@cnu.edu.cn

1947-7988/2018/$25.00

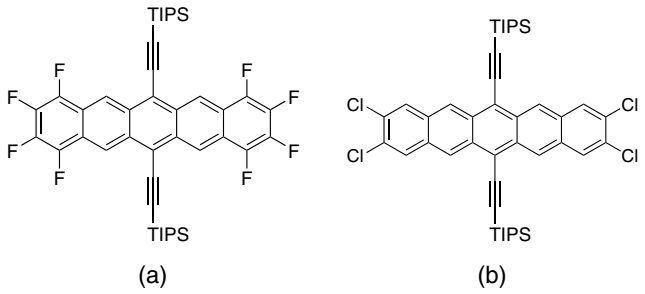

Fig. 1 Molecule structure of substituted TIPS-P used in paper: (a) 8F-TIPS-P and (b) 4Cl-TIPS-P.

description, which assumes that the energy levels of all sites in the system follow Gaussian distribution. Therefore, the effects of blending on charge transport are still open questions.

TIPS (triisopropylsilane) substituted pentacene (TIPS-P) derivatives have attracted great research interest due to their tunable structure, good solubility, and resistant to oxidative decomposition.[17–19] Because of the strong $\pi - \pi$ stacking enhanced by the steric hindrance of the large TIPS group, TIPS-P derivatives exhibit excellent crystallinity and a large class of TIPS-P derivatives adopt similar crystal structure pattern, making them appropriate for constructing a homogeneous blending model. In 2010, Sakanoue and Sirringhaus reported that field effect transistor based on TIPS-P exhibits "band-like" charge transport behavior.[20] However, further study shows that charges in TIPS-P are localized.[21] In addition, theoretical computation demonstrates that the reorganization energy of TIPS-P (197 meV)[22,23] is significantly greater than that of pentacene (92 meV).[24] These results indicate that TIPS-P system should be studied with hopping model and tunneling enabled charge transfer theory.[25]

In this work, we investigate the blending effect in two model TIPS-P derivatives, [(1,2,3,4,8,9,10,11-octafluoropentacene-6,13-diyl)bis(ethyne-2,1-diyl)]bis(triisopropylsilane) (8F-TIPS-P) and [(2,3,9,10-tetrachloropentacene-6,13-diyl)bis(ethyne-2,1-diyl)]bis(triisopropylsilane) (4Cl-TIPS-P), based on *ab initio* DFT calculation and tunneling enabled hopping theory coupled with kinetic Monte-Carlo simulation. The chemical structure of the two molecules is shown in Fig. 1. To model blending systems, the two molecules are mixed homogeneously with continuous ratio, and kinetic Monte-Carlo simulations are performed for each ratio to gain full insight of the relationship between blending ratio and mobility. The system is also evaluated at different temperatures, which is demonstrated to be of great significance to the mobility–blend ratio dependency.

2 Methodology

2.1 *Model Setup*

Among moderately substituted TIPS-P derivatives, which are assumed to have a similar crystal structure pattern, 8F-TIPS-P and 4Cl-TIPS-P are chosen as two model compounds, because the two molecules have relatively compatible energy levels. Their high symmetry also simplifies our calculation without any compromises in accuracy. In the blending model, the two molecules are blended homogeneously based on the reported crystal structure of 8F-TIPS-P determined by XRD.[26] As the ratio of 4Cl-TIPS-P increases from 0 to 1, 4Cl-TIPS-P would randomly replace 8F-TIPS-P, until all 8F-TIPS-P molecules become 4Cl-TIPS-P molecules, as shown in Fig. 2. Previous theoretical work has shown that 8F-TIPS-P is n-type semiconductor and an isomer of

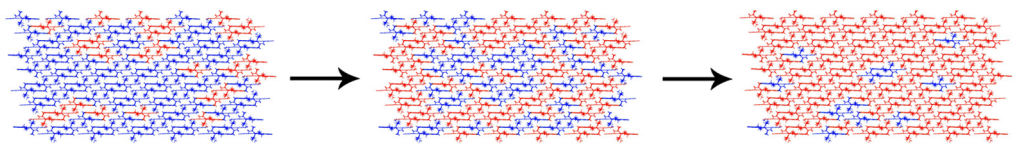

Fig. 2 Schematic representation of the random 4Cl-TIPS-P (red) substitution in 8F-TIPS-P (blue) crystal structure. The substitution ratio is 0.2, 0.5, and 0.8, respectively.

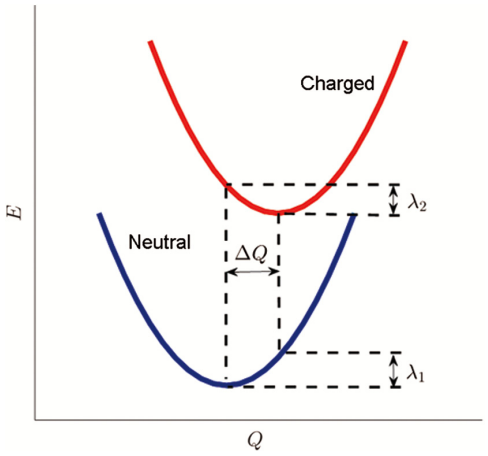

Fig. 3 Schematic representation of the potential energy surfaces of the neutral and charged states with respect to the reaction coordinate.

the 4Cl-TIPS-P is ambipolar semiconductor.[23] Thus, our calculation will only focus on electron transport in the organic semiconductors.

2.2 *Transfer Integral, Reorganization Energy, and Site Energy Difference*

Many methods have been proposed on the calculation of transfer integral, such as energy splitting method,[27–29] the site energy correction method,[30–32] the direct coupling method,[24,33,34] constrained DFT,[35,36] super-exchange coupling,[37] and so on. Theoretical studies have shown that the frontier energy levels of functionalized TIPS-Ps usually distribute within a range of 0.6 eV, which rules out a donor-acceptor description for the mixed system. In this paper, we adopt the site energy correction method. The method takes the site energy differences into account and has been proven to be reliable and easy to be adopted.[38–41] According to the method, transfer integral between molecule A and B V_{AB} reads

$$V_{AB} = \frac{V_{AB^0} - \frac{1}{2}(\varepsilon_A + \varepsilon_B)S_{AB}}{1 - S_{AB}^2}, \tag{1}$$

where $V_{AB}^0 = \langle \psi_A | H | \psi_B \rangle$, $\varepsilon_A = \langle \psi_A | H | \psi_A \rangle$, and $S_{AB} = \langle \psi_A | \psi_B \rangle$, $\psi_{A(B)}$ is the frontier molecular orbital of the isolated molecule A(B) in the dimer structure, H is the dimer Hamiltonian. The molecular orbital calculation is performed with the Guassian09 Program[42] using PW91PW91/6-31G* level of theory, then transfer integral V is obtained with MOMAP program package developed by our group.

The charge reorganization energy λ consists of two terms. The first term is the energy difference of the neutral molecule in the optimal charged geometry and in the equilibrium neutral geometry, λ_1. The second term is the energy difference of the charged molecule in these two geometries, λ_2, as sketched in Fig. 3. The charge reorganization energy λ can be decomposed into normal mode relaxation energy.[43] The vibration frequencies and the normal coordinates of the neutral and anion single molecules are calculated from optimized geometries using the Gaussian09 program with the B3LYP functional and the 6-31G(d) basis set, then the DUSHIN program is used to calculate the Huang–Rhys factor and reorganization energy for every vibration mode.[44] The total reorganization energy λ is the sum of the relaxation energy of all normal modes. The site energy difference between the two molecules is obtained from the orbital energies of the optimized molecules based on Koopmans' theorem.

2.3 *Charge Transfer Rate and Mobility*

The charge transfer rates between molecule dimers are calculated based on multimode quantum charge transfer rate using MOMAP

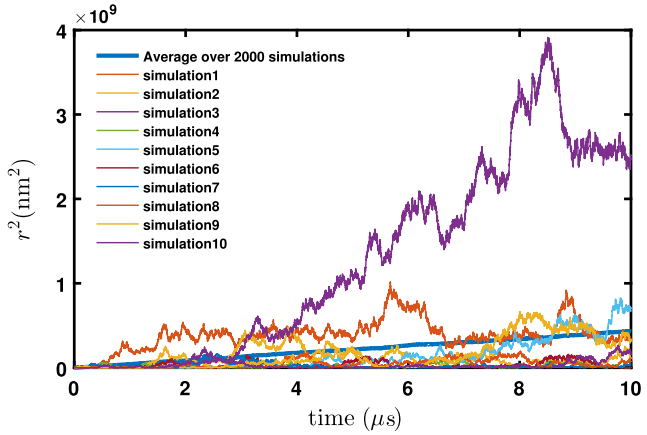

Fig. 4 Squared displacement versus simulation time in a random walk simulation. Each thin solid line represents an individual simulation. The thick solid line means the average over 2000 simulations.

$$k_{fi} = \frac{|V_{fi}|^2}{\hbar^2} \int_{-\infty}^{\infty} \mathrm{d}t \, \exp\left\{ it\omega_{fi} - \sum_j S_j[(2n_j + 1) - n_j e^{-it\omega_j}(n_j + 1)e^{it\omega_j}] \right\}, \tag{2}$$

where k_{fi} is the charge transfer rate between two sites, V_{fi} is the transfer integral, ω_{fi} is the site energy difference, and S_j, ω_j, and n_j are the Huang–Rhys factor, vibration frequency, and phonon occupation number of the j'th vibration mode, respectively. Here, $n_j = 1/[\exp(\frac{\hbar\omega_j}{k_B T}) - 1]$. In the high temperature and short time limits, Eq. (2) yields Marcus rate equation

$$k_{fi} = \frac{|V_{fi}|^2}{\hbar} \sqrt{\frac{\pi}{\lambda k_B T}} \exp\left[-\frac{(\Delta G + \lambda)^2}{4\lambda k_B T} \right]. \tag{3}$$

The mobility of the blending system is obtained based on multimode quantum charge transfer rate through a kinetic Monte-Carlo random walking approach[45]

$$\mu = \frac{eD}{k_B T}, \tag{4}$$

where D is the diffusion coefficient and for an n-dimensional system $D = \frac{1}{2n} \lim_{t\to\infty} \frac{\langle r^2 \rangle}{t}$. Here r is the displacement of charge carrier obtained by random walk through the molecular crystal structure (See Fig. 4). In our simulations, no external electric field is applied. The charge hops between nearest neighbor molecules with a probability $p_i = \frac{k_i}{\Sigma_j k_j}$. At each step, a random number rnd uniformly distributed between 0 and 1 is generated. If $\Sigma_i^{k-1} p_i < rnd \leq \Sigma_i^k p_i$, then the charge is assumed to move to the k'th neighbor. 8F-TIPS-P and 4Cl-TIPS-P form a two-dimensional (2-D) transport network and the average mobility on all directions are used to measure the charge transport property of the material.

3 Results and Discussion

3.1 *Basic Parameters for the Blending System*

The blending system is studied based on the crystal structure of 8F-TIPS-P. In the crystal, molecules are packed layer-by-layer and chemical environments for all molecules are the same, providing us with convenience for modeling as well as for calculation. As shown in Fig. 5, six charge hopping pathways are available for an arbitrary site in the crystal. In view of translation symmetry, sites A and F are equivalent, and sites B, C, D, and E are equivalent. Because of the symmetry, the charge transfer rates of the two pathways between A and F are equal.

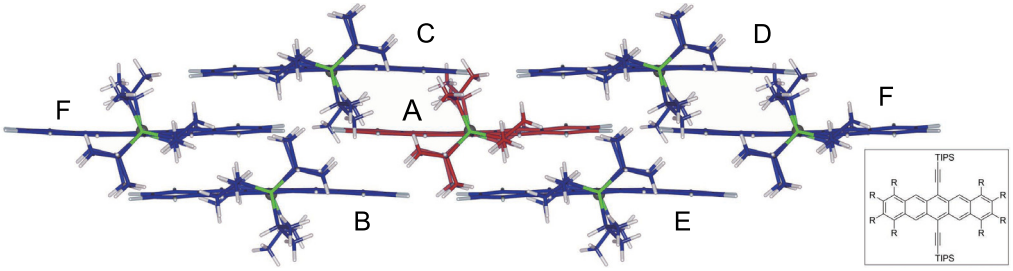

Fig. 5 Six possible charge transfer pathways in 8F-TIPS-P crystal. Red, an arbitrary molecule; Blue, neighbor molecules. Inset: molecule structure of 8F-TIPS-P.

Table 1 Transfer integral V(meV) between 8F-TIPS-P (8F) and 4Cl-TIPS-P (4Cl).

	Type of the start and end molecules			
Pathway	8F → 8F	8F → 4Cl	4Cl → 8F	4Cl → 4Cl
A → B	19.3	30.1	30.2	40.0
A → C	0.7	8.1	8.0	15.6
A → D	0.4	6.8	6.8	10.5
A → E	130.2	150.9	150.9	170.3
A → F	0.4	4.5	4.5	25.3

As it is possible for 4Cl-TIPS-P to substitute any sites in the crystal structure, the terminal residue molecules of the five kinds of charge hopping pathways could either be 8F-TIPS-P or 4Cl-TIPS-P, i.e., charge may hop from 8F-TIPS-P to 8F-TIPS-P, 8F-TIPS-P to 4Cl-TIPS-P, 4Cl-TIPS-P to 8F-TIPS-P, or 4Cl-TIPS-P to 4Cl-TIPS-P, producing 20 different pairs of charge hopping pathways. The transfer integrals of the 20 pathways are listed in Table 1, which shows some trends worth noticing: (a) no matter what kinds of molecules are in the start and end of the hopping pathway, V between A and E (noted as V_{AE}, the same hereinafter) is the greatest. From chemical instinct, V_{AE} and V_{AC} should be approximately the same; however, molecule A is not symmetric of the plane, leading to a great difference between V_{AE} and V_{AC}. Fan et al. demonstrated the trend as well.[23] (b) Because of the high symmetry and similarity of 8F-TIPS-P and 4Cl-TIPS-P, for a certain pathway, switching the two residue molecules have a negligible effect to transfer integrals. If a much different or nonsymmetric molecule is introduced to the crystal and the central symmetry of the molecular pair is broken, a significant difference upon switching the molecules is expected. (c) Transfer integral tends to increase as the chlorine substitution increases, which could be attribute to the more expanded chlorine orbitals; however, it should be noted that the unoptimized crystal structure may lead to an overestimation of V involving 4Cl-TIPS-P.

The reorganization energy of 8F-TIPS-P and 4Cl-TIPS-P calculated by normal mode analysis method is shown in Table 2. λ_1 represents the neutral state and λ_2 represents the anion state. Figure 6 further shows the contribution of each normal mode to the reorganization energy. We found that although the two molecules are rather similar in molecular weight or number of electrons, their reorganization energy and normal vibration modes differ considerably. This is probably because different substitutions affect the LUMO representing electron.[46] For $\lambda(8F-TIPS-P)$, especially λ_2, vibrational modes with lower frequency contribute more, whereas for 4Cl-TIPS-P, high frequency modes are of greater significance. Vibration modes with most contributions to the reorganization energy for the two molecules are both related to in-plane double bond stretching in the core.

The ΔG of the electron transfer process from 8F-TIPS-P to 4Cl-TIPS-P is determined to be 48.1 meV according to Koopmans' theorem. Using this value as the site energy difference for

Table 2 Reorganization energy λ of 8F-TIPS-P and 4Cl-TIPS-P.

	Reorganization energy λ (meV)		
Molecule type	λ_1 (neutral)	λ_2 (anion)	λ
8F-TIPS-P	121	131	252
Cl-TIPS-P	93	95	188

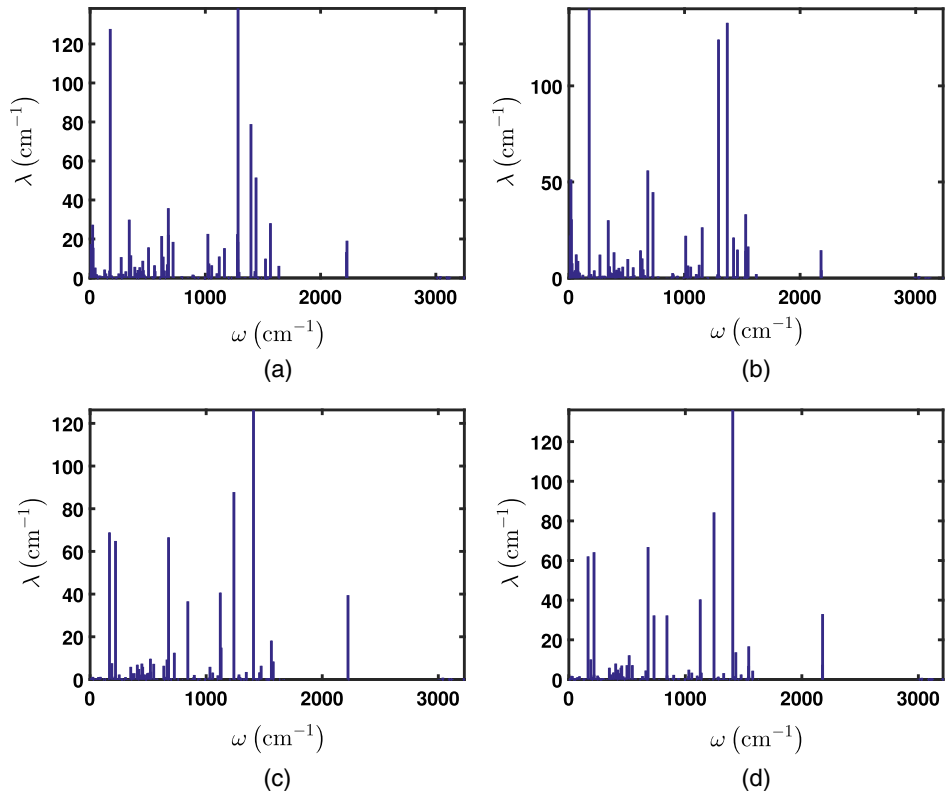

Fig. 6 Reorganization energy of 8F-TIPS-P and 4Cl-TIPS-P from NM analysis: (a) $\lambda_1(8F-TIPS-P)$, (b) $\lambda_2(8F-TIPS-P)$, (c) $\lambda_1(4Cl-TIPS-P)$, and (d) $\lambda_2(4Cl-TIPS-P)$. λ_1 represents the neutral state and λ_2 represents the anion state.

the two molecules, 20 pairs of charge transfer rate k were calculated based on tunneling enabled charge transfer theory. The results are shown in Table 3, which exhibits a similar trend with that of V. The main difference is that electron transfer from 8F-TIPS-P to 4Cl-TIPS-P is much slower than the transfer rate on the opposite direction because site energy difference hampers the process. Although electronic transfer from 4Cl-TIPS-P to 8F-TIPS-P is favored energetically and thus accelerated, 4Cl-TIPS-P self-exchange process is generally faster owing to larger V. The charge transfer rates calculated with semiclassical Marcus equation are also listed in the last row of Table 3. For simplicity only k for A → B pathway is shown; however, their smaller value compared to quantum transfer rate result is sufficient to demonstrate that quantum nuclear tunneling effect not negligible at room temperature.

We further set out to explore how k behaves when T changes from 50 to 300 K for all four pairs of start and end molecules taking k_{AE} as an example. Figure 7(a) shows that k for 8F-TIPS-P pair increases with T, in accordance with larger $\lambda(8F-TIPS-P)$ and lower frequency vibration modes. Figure 7(b) implies k from 8F-TIPS-P to 4Cl-TIPS-P is also thermal-activated; however, upon cooling, k is reduced to 0 dramatically, as a result of higher site energy at

Table 3 Charge transfer rate (s^{-1}) between 8F-TIPS-P (8F) and 4Cl-TIPS-P (4Cl).

	Type of the start and end molecules			
Pathway	8F → 8F	8F → 4Cl	4Cl → 8F	4Cl → 4Cl
A → B	2.8×10^{12}	2.8×10^{12}	2.0×10^{13}	2.8×10^{13}
A → C	3.6×10^{9}	2.0×10^{11}	1.4×10^{12}	4.3×10^{12}
A → D	1.4×10^{9}	1.4×10^{11}	1.0×10^{12}	1.9×10^{12}
A → E	1.3×10^{14}	7.1×10^{13}	5.1×10^{14}	5.1×10^{14}
A → F	1.4×10^{9}	6.0×10^{10}	4.5×10^{11}	1.1×10^{13}
Marcus rate A → B	2.3×10^{12}	1.3×10^{12}	9.3×10^{12}	1.0×10^{13}

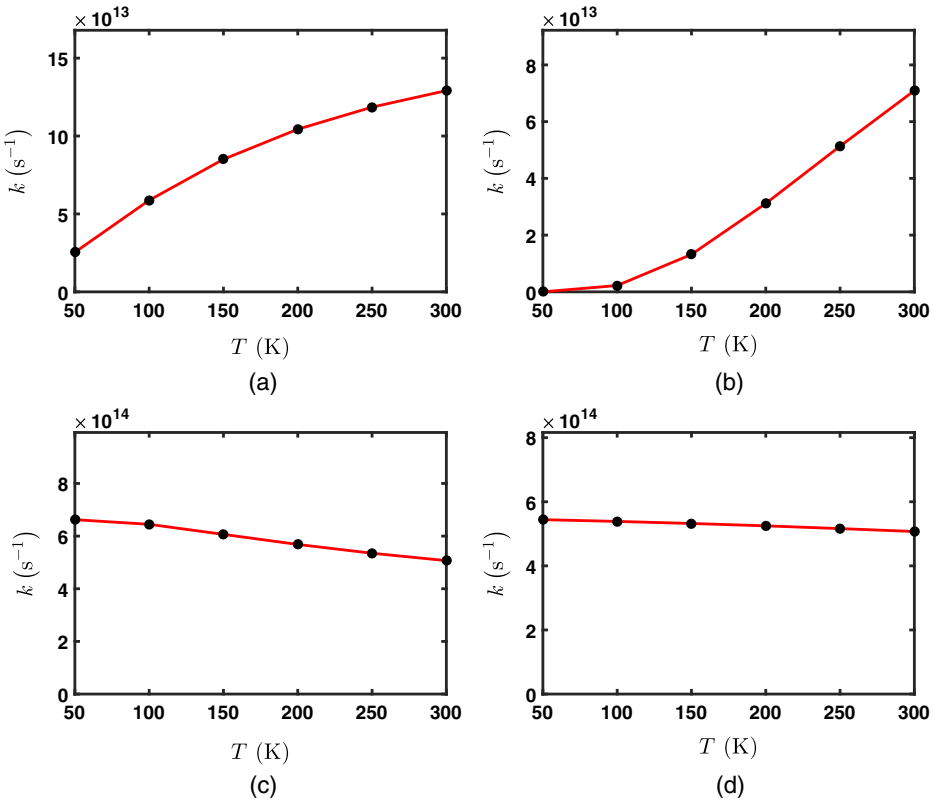

Fig. 7 Temperature dependence of the charge transfer rate between 8F-TIPS-P and 4Cl-TIPS-P: (a) from 8F-TIPS-P to 8F-TIPS-P, (b) from 8F-TIPS-P to 4Cl-TIPS-P, (c) from 4Cl-TIPS-P to 8F-TIPS-P, and (d) from 4Cl-TIPS-P to 4Cl-TIPS-P.

4Cl-TIPS-P. k from 4Cl-TIPS-P to 8F-TIPS-P or 4Cl-TIPS-P decreases as T rises, which could be explained by quantum nuclear tunneling effect.

3.2 *Impact of Blending Ratio and Temperature on Mobility*

The electron mobility of 8F-TIPS-P and 4Cl-TIPS-P blending system can be studied under a temperature ranging from 50 to 300 K through kinetic Monte-Carlo simulation based on the charge transfer rates for all the molecular pairs. The result is shown in Fig. 8(a). First, consider the relationship between μ and T when the ratio of 8F-TIPS-P in the crystal $r = 1$ (pure 8F-TIPS-P)

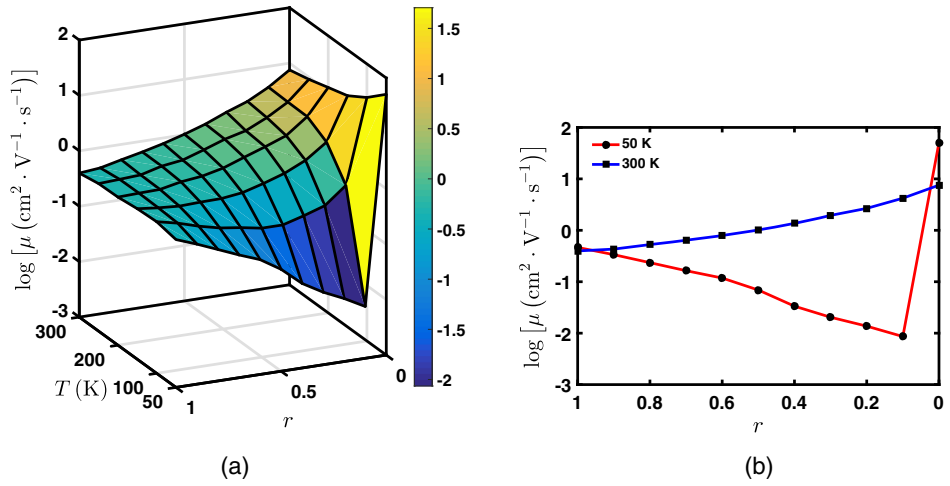

Fig. 8 (a) Ratio of 8F-TIPS-P r and temperature T dependence of the mobility μ of 8F-TIPS-P and 4Cl-TIPS-P blending system. (b) $\mu(r)$ when $T = 50$ and 300 K, respectively. μ axis is logarithmic.

or $r = 0$ (pure 4Cl-TIPS-P). According to the result of the simulation, μ for 8F-TIPS-P does not alter much with temperature change, whereas μ for 4Cl-TIPS-P is negatively correlated with T. The phenomenon could be explained by Fig. 7(a), Fig. 7(d), and Eq. (4), which indicates that the effect of T cancels out for 8F-TIPS-P and facilitates a high mobility at a low temperature for 4Cl-TIPS-P. The mobility obtained with semiclassical transfer rate for pure 8F-TIPS-P and 4Cl-TIPSP-P at 300 K is 0.32 cm^2 and 2.7 $cm^2 \cdot V^{-1} \cdot s^{-1}$, respectively, in contrast to quantum charge transfer mobility of 0.40 cm^2 and 7.6 $cm^2 \cdot V^{-1} \cdot s^{-1}$, indicating 4Cl-TIPS-P system has a stronger nuclear tunneling effect than 8F-TIPSP-P system, in agreement with our analysis of normal modes and charge transfer rates. Then, consider the impact of blending ratio r on μ when $T = 50$ K and $T = 300$ K, which is further shown in Fig. 8(b) for clarity. In the case of $T = 300$ K, as r decreases from 1 to 0 and the crystal transforms from pure 8F-TIPS-P to pure 4Cl-TIPS-P, the mobility shifts smoothly from μ of 8F-TIPS-P to μ of 4Cl-TIPS-P and log μ is basically linear with r. In sharp contrast, when $T = 50$ K, as 4Cl-TIPS-P substitutes more sites in 8F-TIPS-P crystal, μ would first slowly decrease and reach a global minimum when $r \to 0$, then rise discretely to a global maximum, i.e., the μ for pure 4Cl-TIPS-P. A similar trend has been observed experimentally in the zinc phthalocyanine system[10] and other systems, which were analyzed with GDM.[47]

To further investigate the unexpected large $\frac{\partial \mu}{\partial r}$, we performed more simulations for μ at lower T when $r \to 0$. The results are shown in Fig. 9. When $T = 100$ K, mixing 3% of 8F-TIPS-P in 4Cl-TIPS-P would reduce μ by one order of magnitude, whereas when $T = 50$ K, mixing 0.1% of 8F-TIPS-P in 4Cl-TIPS-P would reduce μ by two orders of magnitude. The reason that minor 8F-TIPS-P doping would significantly alter the μ of 4Cl-TIPS-P is that the LUMO of 8F-TIPS-P

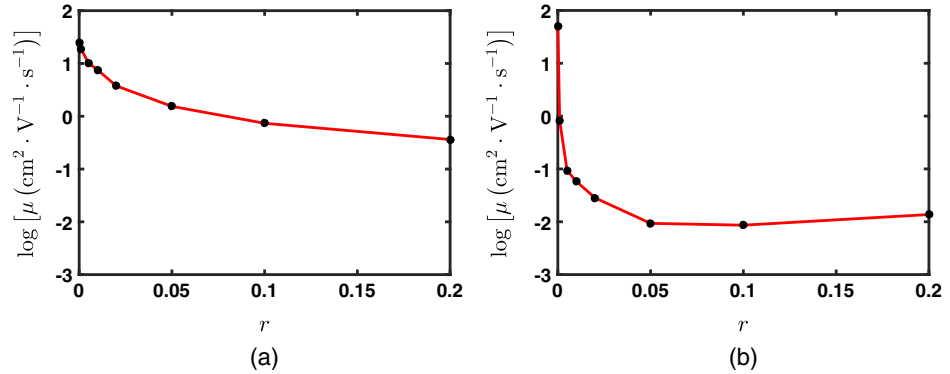

Fig. 9 Ratio of 8F-TIPS-P r dependence of μ when (a) $T = 100$ K and (b) $T = 50$ K.

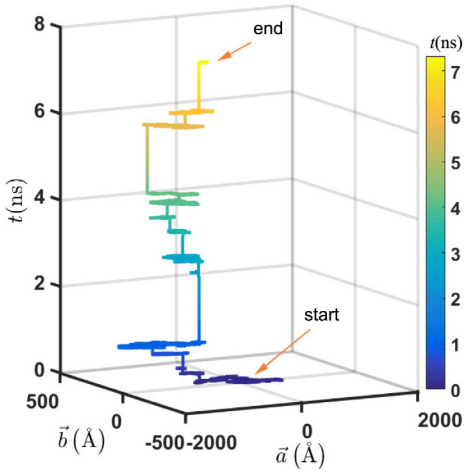

Fig. 10 Displacement ($\vec{a}$ and $\vec{b}$ axis) and time (t axis) relationship in a single random walk simulation when $T = 50$ K and $r = 0.001$.

lays between the HOMO and LUMO of 4Cl-TIPS-P, thus becomes trap for electrons. Because the electron transfer from 8F-TIPS-P to 4Cl-TIPS-P is energetically unfavored, it is extremely difficult at a low temperature. In fact, the k for electron transfer from 8F-TIPS-P to 4Cl-TIPS-P at 50 K is only about one ten-thousandth of that at 300 K, as shown in Fig. 7(b). Thus, 8F-TIPS-P behaves like electron trap for $r \to 0$. When the portion of 8F-TIPS-P further rises, it is possible for charge carriers to hop between "trap" sites, so μ reaches a minimum and then levels off and finally increases to pure 8F-TIPS-P. We note that the mechanism provides an explanation for the experimentally observed nonmonotonic $\mu - T$ relationship, in which upon rising temperature μ would first increase then decrease:[20,48–50] at a low temperature, transport is limited by traps induced by impurities, and increasing T leads to higher μ, whereas at a high temperature, increasing T would reduce μ because of the nuclear tunneling effect.

One advantage of Monte-Carlo simulation is that it provides clear microscopic image to the effect of interest. Figure 10 gives the displacement ($\vec{a}$ and $\vec{b}$ axis) and time (t axis) relationship in a single random walk simulation when $T = 50$ K and $r = 0.001$. As substituted TIPS-P systems are 2-D transport materials, we choose a set of orthogonal bases in the charge transport plane, $\vec{a}$ and $\vec{b}$, to represent the displacement of the charge carrier. We found that there are two types of displacement–time relationship in such a simulation. The first one is platform-like ($\frac{\Delta\|\vec{a}+\vec{b}\|}{\Delta t} \to \infty$), which corresponds to the charge transport in vast range of 4Cl-TIPS-P molecules. The second one is step-like ($\frac{\Delta\|\vec{a}+\vec{b}\|}{\Delta t} \to 0$), which corresponds to the situation where charge carrier is trapped in 8F-TIPS-P molecule.

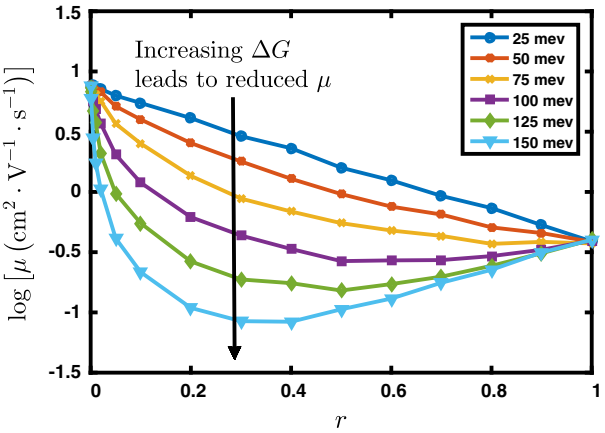

Fig. 11 Dependence of μ on r when $\Delta G = 25$, 50, 75, 100, 125, and 150 meV, respectively.

It is intriguing how the site energy difference between the two molecules ΔG affects $\mu(r)$. We set ΔG to values ranging from 25 to 150 meV with other parameters fixed (specifically, $T = 300$ K) and studied $\mu(r)$ in these conditions. The result shown in Fig. 11 indicates that blending tends to reduce μ with increased ΔG. The origin of this phenomenon is the positive correlation between trap depth and ΔG. When ΔG is large, the charge transfer rate between energetically favored and unfavored directions vary dramatically, charge carriers are prone to stay in traps. Whereas when ΔG is small, trapping effect is unimportant, the blended system behaves like a simple mixture.

4 Conclusion

To conclude, the blending effect in organic semiconductors is studied utilizing the 8F-TIPS-P and 4Cl-TIPS-P homogeneous mixing model and the quantum nuclear tunneling theory. It takes both site energy difference ΔG and disorders in transfer integral into account, to consider $\mu(r)$ as a function of temperature T and ΔG. With higher T and lower ΔG, the mobility of the blended system could be regarded as a linear combination of the two individual components. However, with lower T and higher ΔG, the charge transfer rate from 8F-TIPS-P to 4Cl-TIPS-P becomes several orders lower than that of the opposite direction, and 8F-TIPS-P molecules practically act as traps, which seriously hamper the charge transfer process even when the ratio seems negligible. Our calculations suggest when $T = 50$ K and $\Delta G = 48.1$ meV, blending 0.005 mol. % of 8F-TIPS-P into 4Cl-TIPS-P can reduce the mobility by three orders of magnitude. At room temperature, the trapping effect becomes prominent when ΔG is larger than 100 meV.

Acknowledgments

The authors gratefully acknowledge financial support from the National Key R&D program of China (2017YFA0204702), the National Natural Science Foundation of China (Grant No. 21404067), and the Strategic Priority Research Program of the Chinese Academy of Sciences (Grant No. XDB12020200). The computational work has been carried out in the Tsinghua University High Performance Computing Centre. The authors declare no conflicts of interest. Z. S. has been inspired by Valy's scientific work since 30 years ago. On the occasion of his 70th anniversary, he likes to express his sincere wishes for good health, longevity, happiness, robustness, and more inspiring science.

References

1. M. L. Tang and Z. Bao, "Halogenated materials as organic semiconductors," *Chem. Mater.* **23**, 446–455 (2011).
2. M. L. Tang et al., "Chlorination: a general route toward electron transport in organic semiconductors," *J. Am. Chem. Soc.* **131**, 3733–3740 (2009).
3. M. Brendel et al., "The effect of gradual fluorination on the properties of F_nZnPc thin films and F_nZnPc/C_{60} bilayer photovoltaic cells," *Adv. Funct. Mater.* **25**, 1565–1573 (2015).
4. J. Zhang et al., "Switching charge-transfer characteristics from p-type to n-type through molecular doping (cocrystallization)," *Chem. Sci.* **7**, 3851–3856 (2016).
5. Y.-Q. Sun et al., "Charge-transfer emission of mixed organic cocrystal microtubes over the whole composition range," *Chem. Mater.* **27**, 1157–1163 (2015).
6. B. Lüssem et al., "Doped organic transistors," *Chem. Rev.* **116**, 13714–13751 (2016).
7. H. Jiang et al., "Molecular crystal engineering: tuning organic semiconductor from p-type to n-type by adjusting their substitutional symmetry," *Adv. Mater.* **29**, 1605053 (2017).
8. G. Giri et al., "Tuning charge transport in solution-sheared organic semiconductors using lattice strain," *Nature* **480**, 504–508 (2011).
9. Y. Diao et al., "Solution coating of large-area organic semiconductor thin films with aligned single-crystalline domains," *Nat. Mater.* **12**, 665–671 (2013).
10. M. Schwarze et al., "Band structure engineering in organic semiconductors," *Science* **352**, 1446–1449 (2016).

11. H. Fong, K. Lun, and S. So, "Hole transports in molecularly doped triphenylamine derivative," *Chem. Phys. Lett.* **353**, 407–413 (2002).
12. K. K. Tsung and S. So, "Carrier trapping and scattering in amorphous organic hole transporter," *Appl. Phys. Lett.* **92**, 103315 (2008).
13. B. Li et al., "Effects of carrier trapping and scattering on hole transport properties of *N*, *N*′-diphenyl-*N*, *N*′-bis(1-naphthyl)-1, 1′-biphenyl-4, 4′-diamine thin films," *Org. Electron.* **12**, 974–979 (2011).
14. C. Li et al., "Charge transport in mixed organic disorder semiconductors: trapping, scattering, and effective energetic disorder," *J. Phys. Chem. C* **116**, 19748–19754 (2012).
15. C. Li et al., "Universal trap effect in carrier transport of disordered organic semiconductors: transition from shallow trapping to deep trapping," *J. Phys. Chem. C* **118**, 10651–10660 (2014).
16. H. B. Assler, "Charge transport in disordered organic photoconductors a Monte Carlo simulation study," *Phys. Status Solidi B* **175**, 15–56 (1993).
17. J. E. Anthony et al., "Functionalized pentacene: improved electronic properties from control of solid-state order," *J. Am. Chem. Soc.* **123**, 9482–9483 (2001).
18. J. E. Anthony, D. L. Eaton, and S. R. Parkin, "A road map to stable, soluble, easily crystallized pentacene derivatives," *Org. Lett.* **4**, 15–18 (2002).
19. C. D. Sheraw et al., "Functionalized pentacene active layer organic thin-film transistors," *Adv. Mater.* **15**, 2009–2011 (2003).
20. T. Sakanoue and H. Sirringhaus, "Band-like temperature dependence of mobility in a solution-processed organic semiconductor," *Nat. Mater.* **9**, 736–740 (2010).
21. J.-F. Chang et al., "Hall-effect measurements probing the degree of charge-carrier delocalization in solution-processed crystalline molecular semiconductors," *Phys. Rev. Lett.* **107**, 066601 (2011).
22. R.-M. Wu et al., "Theoretical investigations on electronic and charge transport properties of novel organic semiconductors: triisopropylsilylethynyl(tips)-functionalized anthradifuran and anthradithiophene derivatives," *Comput. Theor. Chem.* **1046**, 107–117 (2014).
23. J.-X. Fan et al., "Theoretical study on charge transport properties of intra- and extra-ring substituted pentacene derivatives," *J. Phys. Chem. A* **120**, 2390–2400 (2016).
24. G. Nan et al., "Nuclear tunneling effects of charge transport in rubrene, tetracene, and pentacene," *Phys. Rev. B* **79**, 115203 (2009).
25. Z. Shuai, L. Wang, and Q. Li, "Evaluation of charge mobility in organic materials: from localized to delocalized descriptions at a first-principles level," *Adv. Mater.* **23**, 1145–1153 (2011).
26. C. R. Swartz et al., "Synthesis and characterization of electron-deficient pentacenes," *Org. Lett.* **7**, 3163–3166 (2005).
27. B. P. Paulson et al., "Investigation of through-bond coupling dependence on spacer structure," *J. Am. Chem. Soc.* **118**, 378–387 (1996).
28. F. C. Grozema et al., "Intramolecular charge transport along isolated chains of conjugated polymers: effect of torsional disorder and polymerization defects," *J. Phys. Chem. B* **106**, 7791–7795 (2002).
29. J.-L. Brédas et al., "Charge-transfer and energy-transfer processes in π-conjugated oligomers and polymers: a molecular picture," *Chem. Rev.* **104**, 4971–5004 (2004).
30. K. Senthilkumar et al., "Charge transport in columnar stacked triphenylenes: effects of conformational fluctuations on charge transfer integrals and site energies," *J. Chem. Phys.* **119**, 9809–9817 (2003).
31. V. Lemaur et al., "Charge transport properties in discotic liquid crystals: a quantum-chemical insight into structure–property relationships," *J. Am. Chem. Soc.* **126**, 3271–3279 (2004).
32. E. F. Valeev et al., "Effect of electronic polarization on charge-transport parameters in molecular organic semiconductors," *J. Am. Chem. Soc.* **128**, 9882–9886 (2006).
33. A. Troisi and G. Orlandi, "Hole migration in DNA: a theoretical analysis of the role of structural fluctuations," *J. Phys. Chem. B* **106**, 2093–2101 (2002).
34. X. Yang et al., "Influences of crystal structures and molecular sizes on the charge mobility of organic semiconductors: oligothiophenes," *Chem. Mater.* **20**, 3205–3211 (2008).

35. Q. Wua, B. Kaduk, and T. V. Voorhisb, "Constrained density functional theory based configuration interaction improves the prediction of reaction barrier heights," *J. Chem. Phys.* **130**, 034109 (2009).
36. B. Maiti et al., "Enhancing charge mobilities in organic semiconductors by selective fluorination: a design approach based on a quantum mechanical perspective," *Chem. Sci.* **8**, 6947–6953 (2017).
37. H. Geng et al., "Understanding the charge transport and polarities in organic donor-acceptor mixed-stack crystals: molecular insights from the super-exchange couplings," *Adv. Mat.* **27**, 1443–1449 (2015).
38. L. Wang et al., "Multiscale study of charge mobility of organic semiconductor with dynamic disorders," *Phys. Chem. Chem. Phys.* **12**, 3309–3314 (2010).
39. C. Wang et al., "Semiconducting -conjugated systems in field-effect transistors: a material odyssey of organic electronics," *Chem. Rev.* **112**, 2208–2267 (2012).
40. G. Nan and Z. Li, "Crystal structure versus charge transport in organic single crystals of [1] benzothieno[3, 2-b][1]benzothiophene derivatives from a multiscale theoretical study," *J. Mater. Chem.* **2**, 1447–1456 (2014).
41. L. Lin et al., "Theoretical insights into the charge transport in perylene diimides based n-type organic semiconductors," *Org. Electron.* **13**, 2763–2772 (2012).
42. M. J. Frisch et al., *Gaussian09, Revision E.01.*, Gaussian Inc., Wallingford, Connecticut (2016).
43. V. Coropceanu et al., "Hole- and electron-vibrational couplings in oligoacene crystals: intramolecular contributions," *Phys. Rev. Lett.* **89**, 275503 (2002).
44. J. R. Reimers, "A practical method for the use of curvilinear coordinates in calculations of normal-mode-projected displacements and Duschinsky rotation matrices for large molecules," *J. Chem. Phys.* **115**, 9103–9109 (2001).
45. Z. Shuai et al., "From charge transport parameters to charge mobility in organic semiconductors through multiscale simulation," *Chem. Soc. Rev.* **43**, 2662–2679 (2014).
46. H. Geng et al., "Theoretical study of substitution effects on molecular reorganization energy in organic semiconductors," *J. Chem. Phys.* **135**, 104703 (2011).
47. I. I. Fishchuk et al., "Transition from trap-controlled to trap-to-trap hopping transport in disordered organic semiconductors," *Phys. Rev. B* **73**, 115210 (2006).
48. N. A. Minder et al., "Band-like electron transport in organic transistors and implication of the molecular structure for performance optimization," *Adv. Mater.* **24**, 503–508 (2012).
49. Y. Krupskaya et al., "Band-like electron transport with record-high mobility in the TCNQ family," *Adv. Mater.* **27**, 2453–2458 (2015).
50. X. Xu et al., "Electron mobility exceeding 10 $cm^2 V^{-1} s^{-1}$ and band-like charge transport in solution-processed n-channel organic thin-film transistors," *Adv. Mater.* **28**, 5276–5283 (2016).

Biographies for the authors are not available.